

1,3,4-Oxadiazole-Containing Histone Deacetylase Inhibitors: Anticancer Activities in Cancer Cells

Sergio Valente,[†] Daniela Trisciuglio,[‡] Teresa De Luca,[‡] Angela Nebbioso,[§] Donatella Labella,[†] Alessia Lenoci,[†] Chiara Bigogno,^{||} Giulio Dondio,^{||} Marco Miceli,[§] Gerald Brosch,[⊥] Donatella Del Bufalo,[‡] Lucia Altucci,^{§,#} and Antonello Mai^{*,†,∇}

[†]Department of Drug Chemistry and Technologies, Sapienza University of Rome, P. le A. Moro 5, 00185 Rome Italy

[‡]Regina Elena National Cancer Institute, Via Elio Chianesi, 53, 00144 Rome, Italy

[§]Department of Biochemistry, Biophysics and General Pathology, Second University of Naples, Vico L. De Crechchio 7, 80138 Naples, Italy

^{||}Aphad Srl, Via della Resistanza 65, 20090 Buccinasco, Milan, Italy

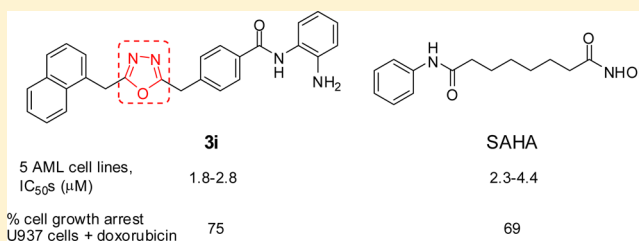
[⊥]Division of Molecular Biology, Biocenter, Innsbruck Medical University, Innrain 80/III, 6020 Innsbruck, Austria

[#]CNR-IGB, Institute of Genetics and Biophysics, via P. Castellino, 80100 Naples, Italy

[∇]Istituto Pasteur-Fondazione Cenci Bolognetti, Sapienza University of Rome, P. le A. Moro 5 00185, Rome, Italy

Supporting Information

ABSTRACT: We describe 1,3,4-oxadiazole-containing hydroxamates (**2**) and 2-aminoanilides (**3**) as histone deacetylase inhibitors. Among them, **2t**, **2x**, and **3i** were the most potent and selective against HDAC1. In U937 leukemia cells, **2t** was more potent than SAHA in inducing apoptosis, and **3i** displayed cell differentiation with a potency similar to MS-275. In several acute myeloid leukemia (AML) cell lines, as well as in U937 cells in combination with doxorubicin, **3i** showed higher antiproliferative effects than SAHA.



INTRODUCTION

Lysine acetylation and deacetylation are crucial post-translational modifications in the epigenetic field. These processes are regulated by two groups of enzymes with opposite activities: histone acetyltransferases (HATs) and histone deacetylases (HDACs), leading to gene transcription or silencing, respectively.¹ Apart from histone modification, HATs and HDACs regulate the post-translational acetylation of many nonhistone proteins, including transcription factors, chaperones, and signaling molecules, resulting in changes in protein stability, protein–protein interactions, and protein–DNA interactions.²

At least 50 nonhistone proteins have been identified as HDAC substrates, including transcription factors (p53, E2F, c-Myc, nuclear factor- κ B (NF- κ B), hypoxia-inducible factor 1 α (HIF-1 α), estrogen receptor α (ER α), and the androgen receptor (AR), MyoD, chaperones (HSP90), signaling mediators (Stat3 and Smad7), and DNA repair proteins.²

HDAC inhibitors (HDACi) mediate cancer cell death through several pathways, and in particular class I HDAC inhibitors are able to induce apoptosis, differentiation, cell cycle arrest, inhibition of DNA repair, upregulation or reactivation of silenced tumor suppressors, downregulation of growth factors, oxidative stress, autophagy, and control of angiogenesis.^{3,4}

A number of HDAC inhibitors are undergoing extensive clinical evaluation as single agents and in combination with other chemotherapeutics; among them, vorinostat (SAHA) and romidepsin (FK-228) have been approved by the U.S. FDA for the treatment of refractory cutaneous T-cell lymphoma (CTCL).^{5,6} In addition, valproic acid (VPA), panobinostat (LBH589), belinostat (PDX101), givinostat (ITF2357), resminostat (4SC-201), entinostat (MS-275), mocetinostat (MGCD0103), 4SC-202, and CHR-3996 (Chart 1) are into phase I/II/III clinical trials alone or in combination with other drugs for treatment of hematological and/or solid tumors.⁴

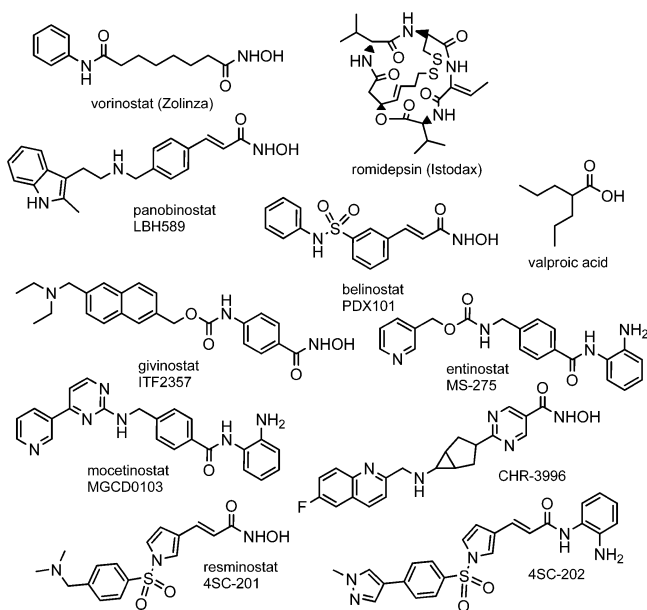
The pharmacophore model for HDACi includes a cap group (CAP) interacting with the rim of the catalytic tunnel of the enzyme, a polar connection unit (CU) linked to a hydrophobic spacer (HS) which allows the molecule to lie into the tunnel, and a Zn-binding group (ZBG) able to complex the Zn²⁺ at the bottom of the cavity.⁷ To date, many different CAP, CU, HS, and ZBG moieties have been studied, and structurally diverse HDAC inhibitors have been recently reviewed.⁸

Since 2001, we described various chemically different series of HDACi [aroylpyrrolylhydroxamates (APHAs) and (aryloxopropenyl)pyrrolylhydroxamates,⁹ aroyl/arylamino-

Received: February 25, 2014

Published: June 27, 2014

Chart 1. HDACi Approved by FDA and/or in Clinical Trials



(phenyloxopropenyl)-, and (amidopropenyl)cinnamyl and pyridinylpropenoic hydroxamates and 2-aminoanilides,¹⁰ and uracil-based hydroxamates and 2-aminoanilides (UBHAs)¹¹] according to the known pharmacophore model. Among them, when tested in human leukemia U937 cells, some acylaminocinnamyl hydroxamates and 2-aminoanilides **1** (Figure 1)

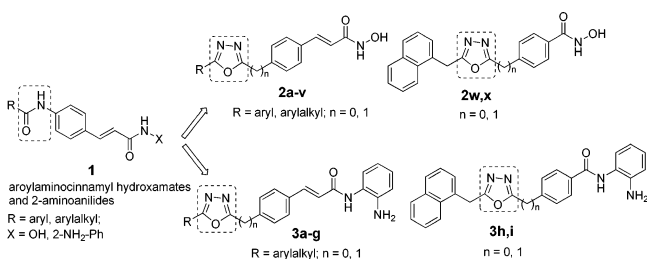


Figure 1. Design of 1,3,4-oxadiazole-containing HDAC inhibitors **2** and **3**.

displayed higher pro-apoptotic and/or cytodifferentiating effects than vorinostat, entinostat, and S-HDAC42, used as reference drugs.¹⁰ Prompted by these results, to study the effect of changes at CU in such compounds, we replaced the amide group of **1** with the bioisostere 1,3,4-oxadiazole moiety, thus developing new series of hydroxamates **2** and 2-aminoanilides **3** (Figure 1), which have been tested as HDACi to assess their capability to induce cell cycle arrest, apoptosis, and/or cytodifferentiation in human leukemia U937 cells. Afterward, selected compounds have been tested in a panel of cancer cells to detect their effects on antiproliferation. Lastly, combination treatment of selected HDACi with doxorubicin in U937 cells have been evaluated.

CHEMISTRY

Cyclocondensation of the hydrazides **5** or **9** (**5a** and **9** are commercially available, **5b** was prepared by reaction between the methyl-4-iodophenylacetate **4** and hydrazine monohydrate in methanol at 60 °C) with the appropriate carboxylic acids provided the iodophenylloxadiazoles **6a–v** or the methyl 1,3,4-

oxadiazol-yl-benzoates **10a,b**, respectively (Scheme 1 and Scheme S1 in Supporting Information). Heck cross-coupling reaction carried out onto the iodo-intermediates **6a–v** with palladium acetate, triethylamine, and *n*-butyl acrylate in *N,N*-dimethylacetamide at 110 °C gave the corresponding butyl esters **7a–v**, which were in turn hydrolyzed with 2N potassium hydroxide in ethanol into the related acids **8a–v** (Scheme 1). The methyl esters **10a,b** were hydrolyzed following the same procedure to furnish the related benzoic acids **11a,b** (Scheme S1 in Supporting Information). Such key compounds **8** and **11** were then converted into the corresponding hydroxamates **2a–v** and **2w,x**, respectively, by reaction with ethyl chloroformate/triethylamine followed by addition of *O*-(2-methoxy-2-propyl)-hydroxylamine and final acidic treatment with Amberlyst 15. In addition, **8h,i,r–v** and **11a,b** were treated with benzotriazole-1-yloxytris(dimethylamino)phosphonium hexafluorophosphate (BOP Reagent, Castro's Reagent), *o*-phenylenediamine, and triethylamine in dry *N,N*-dimethylformamide to afford the corresponding 2-aminoanilides **3a–g** and **3h,i**, respectively (Scheme 1 and Scheme S1 in Supporting Information).

Chemical and physical data for the intermediate compounds **5–8**, **10**, and **11** are reported in Supporting Information. Chemical and physical data for the final compounds **2** and **3** are listed in Tables S4 and S5 in Supporting Information.

RESULTS AND DISCUSSION

Enzyme Studies. To perform a first preliminary screening, the hydroxamates **2a–x** were tested by determining their IC₅₀ values against maize HD1-B and HD1-A, two homologues of class I and class II HDACs, and against class I mouse HDAC1 (Tables S8 and S9 in Supporting Information). Afterward, a series of related 2-aminoanilides **3a–i** have been prepared, and selected compounds **2** and **3a–i** were screened against human recombinant HDAC1 and HDAC4 (% of inhibition at 5 μM) using histone H3 (HDAC1) or the nonhistone trifluoroacetyllysine¹² (HDAC4) as a substrate, respectively (Table S10 in Supporting Information). From these preliminary screenings, it emerged that, regardless of bearing an hydroxamate or an anilide function, (i) the introduction of 1-naphthyl ring at the 1,3,4-oxadiazole C5-position provided the highest inhibitory potency, (ii) the insertion of one methylene unit (no more) between the above aryl ring and the C5-position of the oxadiazole increased the potency of the derivatives, and (iii) this potency can be further improved by the introduction of an additional methylene unit between the 1,3,4-oxadiazole C2-position and the cinnamic/benzoic portion.

From these first results, we selected the hydroxamates **2h**, **2r**, **2t**, **2w**, and **2x** as well as the 2-aminoanilides **3a–c**, **3e**, **3h**, and **3i** to determine the IC₅₀ values against human HDAC1, HDAC4, and HDAC6 (Table 1). SAHA was tested as reference drug.

The hydroxamates **2h**, **2r**, **2t**, and **2x** displayed submicromolar (or single-digit micromolar, **2x** vs HDAC6) inhibition toward HDAC1 and HDAC6, while they are much less efficient against HDAC4. The “double methylene space” inserted between the aryl CAP group and the C5-oxadiazole position on one hand, and between the C2-oxadiazole and the cinnamic/benzoic hydroxamate HS-ZBG on the other hand, conferred to the derivatives **2t** and **2x** the highest potency against HDAC1, while the replacement of the cinnamic with the benzoic moiety at the HS led to less effective HDAC6 inhibition (compare **2t** with **2x**). In the 2-aminoanilide series, the change from cinnamic to benzoic linker led to more potent

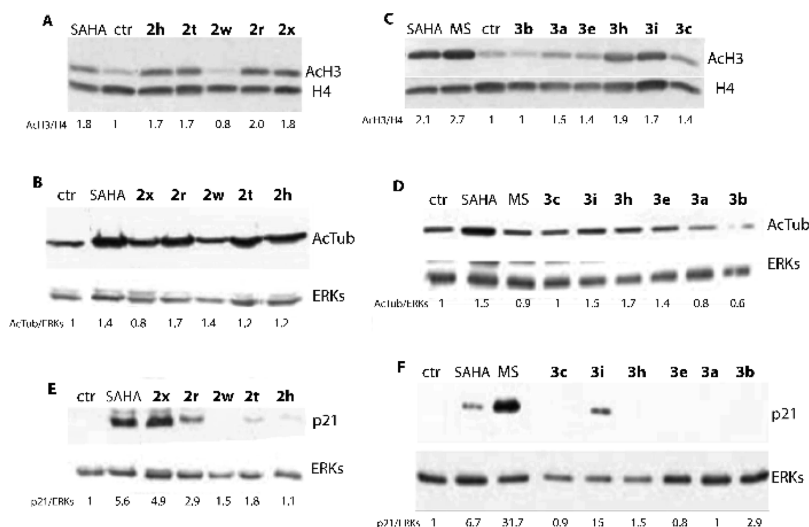


Figure 2. Effects of selected compounds **2** on acetyl-H3 (A) and acetyl- α -tubulin (B) levels in U937 cells. Effects of selected compounds **3** on acetyl-H3 (C) and acetyl- α -tubulin (D) levels in U937 cells. Effect of p21 induction by selected compounds **2** (E) and **3** (F). Western blot analyses were performed with specific antibodies. H4 and ERK proteins were used for equal loading. Blots representative of two independent experiments with similar results are shown. Acetyl-H3, acetyl- α -tubulin, and p21 levels were quantified by densitometric analyses, and fold increase relative to control cells is presented.

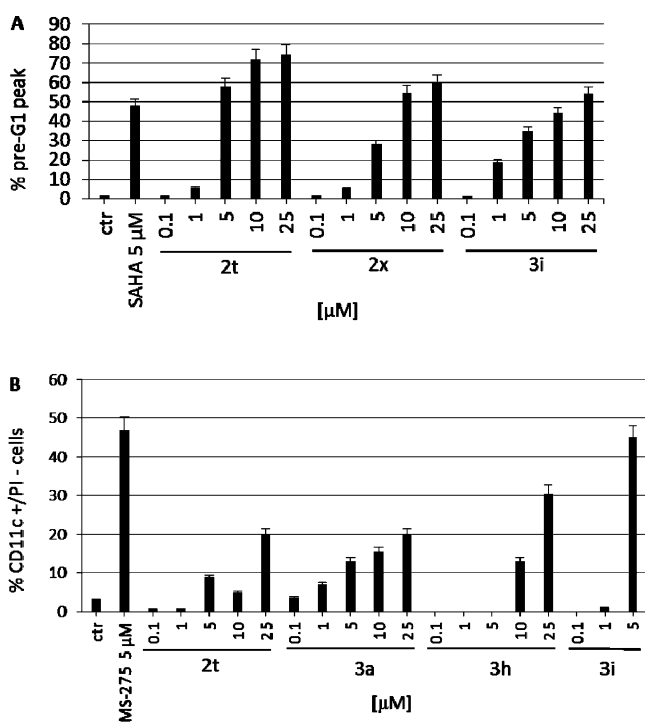


Figure 3. Dose-dependent apoptosis induction (A) and cytodifferentiation (B) in human leukemia U937 cells treated with selected **2** and **3** derivatives.

solubility and high apoptosis so that the differentiation effect was not detectable.

Antiproliferative Activities of 2t and 3i in Cancer Cells. Combination Treatment with Doxorubicin. The hydroxamate **2t** and the 2-aminoanilide **3i** were tested in a panel of different cancer cell lines (lung, colon, liver, and breast cancer, melanoma, osteosarcoma, and leukemias) to determine their antiproliferative activities (Table 2).

In general, the anilide **3i** showed similar or lower IC_{50} values than the hydroxamate **2t** along the various cancer cell lines. The

Table 2. Antiproliferative IC_{50} Values of **2t** and **3i** in a Panel of Cancer Cell Lines^a

cell line	cancer type	$IC_{50} \pm SD$ (μ M)	
		2t	3i
M14	melanoma	45 \pm 8	43.3 \pm 2.9
SANTO	melanoma	24 \pm 6.4	17.4 \pm 3.9
A549	lung	29.5 \pm 9.2	23.6 \pm 1.4
HCT116	colon	21.3 \pm 5.8	24.7 \pm 0.2
SW620	colon	5.1 \pm 0.03	6.7 \pm 1.5
HCC937	breast	33.6 \pm 6.9	29.8 \pm 1.9
MB468	breast	18.4 \pm 6.7	19.6 \pm 5.7
U2OS	osteosarcoma	50 \pm 13.9	20.4 \pm 4
U937	leukemia	7.8 \pm 0.9	1.8 \pm 1.2
HL60	leukemia	6.0 \pm 2.4	2.8 \pm 1.9
HEL	leukemia	4.1 \pm 0.2	2.0 \pm 0.2
KG1	leukemia	2.6 \pm 0.2	1.8 \pm 0.9
MOLM13	leukemia	2.2 \pm 0.1	1.6 \pm 0.6

^aValues represent the mean of at least three separate experiments.

most responsive cancer cell lines were the colorectal adenocarcinoma SW620 and all the tested human acute myeloid leukemia (AML) cell lines (U937, HL60, HEL, KG1, and MOLM13), whose proliferation was inhibited by **3i** and **2t** at single-digit micromolar concentrations. When compared to SAHA, **3i** displayed higher cell growth arrest against all the tested AML U937, HL60, HEL, KG1, and MOLM13 cells (SAHA IC_{50} values: 3.0, 2.9, 2.3, 4.4, and 2.9 μ M, respectively).

Because of their high antiproliferative effects in leukemia, we tested **2t**, **3i**, or SAHA (each at 2.5 μ M) in combination with doxorubicin (0.2 μ M) in U937 for 24 h (Figure 4). In this assay, all the combinations between doxorubicin and HDACi displayed increased cell growth arrest with respect to the treatment with the single agent. Interestingly, the use of doxorubicin plus **3i** was more effective than doxorubicin plus SAHA (75% vs 69% inhibition of proliferation), thus confirming the higher potency of **3i** respect to SAHA.

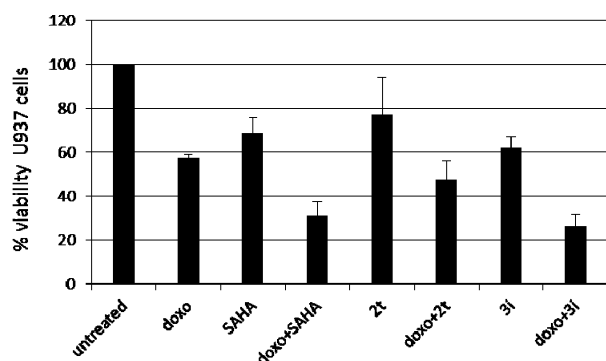


Figure 4. Antiproliferative effect of combination treatment between doxorubicin (0.2 μM) and SAHA, 2t, or 3i (each at 2.5 μM), in U937 cells for 24 h.

CONCLUSIONS

On the basis of structural motifs of the aroylaminocinnamyl hydroxamates and 2-aminoanilides **1** previously described by us and displaying high pro-apoptotic and/or cytodifferentiating effects in human leukemia U937 cells,¹⁰ we planned to replace the amide group (CU) of such compounds with its bioisoster 1,3,4-oxadiazole group and to synthesize a new series of hydroxamates **2** and 2-aminoanilides **3** to be tested as HDACi and anticancer agents.

Among all the prepared hydroxamates **2a–x** and 2-aminoanilides **3a–i**, we selected compounds **2h,r,t,w,x** and **3a–c,e,h,i** to determine their IC_{50} values against human HDAC1, -4, and -6. In general, the hydroxamates **2** were active across 2 out of 3 isoforms where the anilides **3** displayed high inhibition only against HDAC1. In Western blot experiments, the hydroxamates **2** increased both histone H3 and α -tubulin acetylation, while among the anilides, only **3e**, **3h**, and **3i** showed effects on both the targets. About p21 induction, **2r**, **2x**, and **3i** gave a signal at 5 μM , **3i** being more effective than SAHA. When tested in U937 cells for 48 h as pro-apoptotic and/or cytodifferentiation agents, **2t**, **2x**, and **3i** showed a dose-dependent apoptotic effect, **2t** being more potent than SAHA at 5 μM , and **2t**, **3a**, **3h**, and **3i** induced a dose-dependent differentiation determined as increased percentage of CD11c positive/PI negative cells respect to the control. In this assay, at 5 μM , **3i** displayed the same potency as MS-275, one of the most efficient HDACi in cytodifferentiation. When tested against a panel of cancer cell lines to assess their antiproliferative potential, **3i** and **2t** displayed single-digit micromolar activity against SW620 colon adenocarcinoma and five AML cell lines (U937, HL60, HEL, KG1, and MOLM13), **3i** always being more potent than SAHA in leukemias. In combination treatment with doxorubicin, **3i** was more effective than SAHA in inhibiting U937 cell proliferation.

From the data presented, it appears that specific HDAC1 inhibition well correlates with induction of apoptosis, cell differentiation, and cell growth arrest. The anticancer properties showed by **3i**, higher than SAHA in both enzyme (HDAC1) and cellular assays, will be further studied in other cancer contexts.

EXPERIMENTAL SECTION

Chemistry. Melting points were determined on a Buchi 530 melting point apparatus and are uncorrected. ^1H NMR and ^{13}C NMR spectra were recorded at 400 MHz on a Bruker AC 400 spectrometer; chemical shifts are reported in δ (ppm) units relative to the internal

reference tetramethylsilane (Me_4Si). EIMS spectra were recorded with a Fisons Trio 1000 spectrometer; only molecular ions (M^+) and base peaks are given. All compounds were routinely checked by TLC, ^1H NMR, and ^{13}C NMR spectra. TLC was performed on aluminum-backed silica gel plates (Merck DC, Alufolien Kieselgel 60 F254) with spots visualized by UV light. All solvents were reagent grade and, when necessary, were purified and dried by standard methods. Concentration of solutions after reactions and extractions involved the use of a rotary evaporator operating at reduced pressure of ca. 20 Torr. Organic solutions were dried over anhydrous sodium sulfate. Elemental analysis has been used to determine purity of the described compounds, that is, >95%. Analytical results are within $\pm 0.40\%$ of the theoretical values. All chemicals were purchased from Aldrich Chimica, Milan (Italy), or from Alfa Aesar, Karlsruhe (Germany), and were of the highest purity.

General Procedure for the Synthesis of the *N*-Hydroxy-3-(4-(5-aryl/arylalkyl-1,3,4-oxadiazol-2-yl)phenyl)acrylamides and -benzamides (2a–x). Example: *N*-Hydroxy-4-(5-(naphthalen-1-ylmethyl)-1,3,4-oxadiazol-2-yl)methyl)benzamide (**2x**). Triethylamine (1.13 mmol, 0.16 mL) and ethyl chloroformate (1.04 mmol, 0.10 mL) were added to a solution of 4-((5-(naphthalen-1-ylmethyl)-1,3,4-oxadiazol-2-yl)methyl)benzoic acid **11b** (0.87 mmol, 0.3 g) in dry tetrahydrofuran (10 mL) at 0 $^\circ\text{C}$, and the resulting mixture was stirred at this temperature for 15 min. After this time, *O*-(2-methoxy-2-propyl)hydroxylamine (2.61 mmol, 0.19 mL) was added and the mixture was stirred for 1 h. The solvent was evaporated, the residue was eluted with methanol (10 mL), and the ionic resin Amberlyst 15 (25 mg of resin per 0.25 mmol of acid) was added. After 2 h, the resin was filtered off, the product concentrated in vacuo, washed with diethyl ether (3 \times 10 mL), and recrystallized by benzene/acetonitrile. ^1H NMR ($\text{DMSO}-d_6$) δ 4.22 (s, 2H, $-\text{CH}_2$ -naphthalene), 7.34–7.36 (d, 2H, benzene protons), 7.40–7.45 (m, 2H, naphthalene protons), 7.53–7.54 (d, 2H, benzene protons), 7.76–7.78 (m, 2H, naphthalene protons), 7.86–7.88 (d, 1H, naphthalene proton), 7.92–7.94 (d, 1H, naphthalene proton), 8.13 (d, 1H, naphthalene proton), 9.56 (bs, 1H, CONHOH), 10.95 (bs, 1H, CONHOH). ^{13}C NMR ($\text{DMSO}-d_6$) δ 29.2, 30.9, 124.2, 124.3, 125.6, 125.8, 126.5, 126.9, 127.4 (2C), 128.6, 129.2 (2C), 131.2, 132.6, 133.5, 134.0, 139.7, 163.0, 166.4 (2C). MS (EI): m/z [M^+]: 359.1270.

General Procedure for the Synthesis of the *N*-(2-Amino-phenyl)-3-(4-(5-aryl/arylalkyl-1,3,4-oxadiazol-2-yl)phenyl)acrylamides and -Benzamides (3a–i) Example: *N*-(2-Amino-phenyl)-4-((5-(naphthalen-1-ylmethyl)-1,3,4-oxadiazol-2-yl)methyl)benzamide (**3i**). Triethylamine (2.32 mmol, 0.32 mL) and benzotriazole-1-yloxytris(dimethylamino)phosphonium hexafluorophosphate (BOP Reagent) (0.70 mmol, 0.31 g) were added to a solution of 4-((5-(naphthalen-1-ylmethyl)-1,3,4-oxadiazol-2-yl)methyl)benzoic acid **11b** (0.58 mmol, 0.2 g) in anhydrous *N,N*-dimethylformamide (5 mL) under nitrogen atmosphere. The resulting mixture was stirred for 30 min at room temperature, afterward, 1,2-phenylenediamine (0.58 mmol, 0.06 g) was added under nitrogen atmosphere and the mixture was stirred overnight. The reaction was quenched with water (50 mL) and extracted with ethyl acetate (3 \times 30 mL). The combined organic layers were washed with sodium chloride solution (3 \times 20 mL), dried with sodium sulfate, and the residue obtained upon evaporation of solvent was purified by column chromatography (SiO_2 eluting with ethyl acetate/*n*-hexane 1/1) to give pure **3i**. ^1H NMR ($\text{DMSO}-d_6$, 400 MHz, δ ; ppm) δ 4.27 (s, 2H, CH_2 -benzene), 4.67 (s, 2H, $-\text{CH}_2$ -naphthalene), 4.88 (s, 2H, NH_2), 6.59–6.61 (t, 1H, naphthalene proton), 6.76–6.78 (d, 1H, naphthalene proton), 6.96–6.99 (t, 1H, naphthalene proton), 7.14–7.16 (d, 1H, benzene proton), 7.36–7.39 (d, 2H, benzene protons), 7.48–7.52 (d, 2H, naphthalene protons), 7.54–7.57 (m, 2H, benzene proton), 7.87–7.96 (m, 4H, benzene protons and naphthalene protons), 8.06–8.08 (d, 1H, benzene proton), 9.37 (bs, 1H, CONHPh). ^{13}C NMR ($\text{DMSO}-d_6$) δ 29.2, 30.9, 116.5, 119.0, 122.4, 122.9, 124.2, 124.3, 125.2, 125.6, 125.8, 126.5, 126.9, 127.4 (2C), 128.6, 129.2 (2C), 131.2, 132.6, 133.5, 134.0, 139.7, 141.8, 164.8, 166.4 (2C) ppm. MS (EI): m/z [M^+]: 434.1734.

Fluorimetric Human Recombinant HDAC1, -4, and -6 Assays. The HDAC fluorescent activity assay for HDAC1, -4, and

-6 was based on the Fluor de Lys Substrate and Developer combination (BioMol) and has been carried out according to supplier's instructions. First, the inhibitors and purified recombinant HDAC1, HDAC4, or HDAC6 enzymes were preincubated at room temperature for 15 min before substrate addition, the Fluor de Lys Substrate, which comprises an acetylated lysine side chain. For HDAC4 assay, the HDAC4-selective, nonhistone substrate reported by Lahm et al.¹² was used. Full length HDAC1 and HDAC4 fused with a C-terminal His tag were expressed using baculovirus systems. Deacetylation sensitized the substrates that, in the second step, treated with the developer produced a fluorophore. Fluorescence was quantified with a TECAN Infinite M200 station.

Cell Cultures. Human acute myeloid leukemia (AML) cell lines (HL-60, HEL 92.1.7, MOLM-13, KG1, U-937)¹³ were cultured in RPMI with 10% fetal calf serum, 100 U/mL penicillin, 100 µg/mL streptomycin, and 250 ng/mL amphotericin-B, 10 mM HEPES, and 2 mM glutamine. AML cells were kept at the constant concentration of 200 000 cells per milliliter of culture medium. HCT116 and SW620 (colon carcinoma cancer), M14 and SANTO (melanoma), H1299 and A549 (nonsmall-cell lung carcinoma), HCC937 and MB468 (breast carcinoma), and U2OS (osteosarcoma) were cultured in RPMI (Invitrogen) with 10% fetal calf serum (Hyclone), 100 U/mL penicillin.

Western Blot Analysis for α -Tubulin and Histone H3 Acetylation in U937 Cells. For quantification of histone H3 acetylation, 5 mg of total histone extracts were separated on a 15% polyacrylamide gel and blotted as described.¹⁴ Western blots were shown for acetylated histone H3 (Upstate) antibodies, and histone H4 (Abcam) antibodies was used to normalize for equal loading. For determination of α -tubulin acetylation, 25 mg of total protein extracts were separated on a 10% polyacrylamide gel and blotted as described.¹⁵ Western blots were shown for acetylated α -tubulin antibodies (Sigma), and total ERKs (Santa Cruz) were used to normalize for equal loading.

Determination of p21^{WAF1/CIP1} Induction in U937 Cells. Total protein extracts (100 mg) were separated on a 15% polyacrylamide gel and blotted as previously described.^{15,16} Western blots were shown for p21 antibodies (Transduction Laboratories), and total ERKs (Santa Cruz) were used to normalize for equal loading.

Cell Cycle Analysis on U937 Cells. See Supporting Information.

Granulocytic Differentiation on U937 Cells. See Supporting Information.

Antiproliferative Activity in Cancer Cells. Exponentially growing AML and solid tumor cells were seeded in duplicates in 6-well (2 × 10⁵ cells/well) or in sextuplicates in 96-well (3 × 10³ cells/well) and 24 h later cells were treated with SAHA, 2t, and 3i at concentrations ranging from 1 to 50 µM for 48 h. Cell viability of AML and solid tumor cells was evaluated by Cell Titer GLo Assay and by 3-[4,5-dimethylthiazol-2-yl]-2,5-diphenyltetrazolium bromide (MTT, Sigma-Aldrich) assays, respectively, as previously described.^{13,17}

For combination experiments, cells were seeded in duplicated in 6-well and treated with 2.5 µM 2t, 3i, and SAHA alone or in combination with doxorubicin (Doxo, 0.2 µM). Cell viability was analyzed after 24 h of treatment by Cell Titer GLo Assay.

The concentration of 2t and 3i that causes a 50% of cell viability inhibition (IC₅₀) was calculated by CalcuSyn software (Biosoft).

■ ASSOCIATED CONTENT

Ⓢ Supporting Information

Chemical and physical data for compounds 2, 3, 5–8, 10, and 11. HDAC inhibitory assays against maize HD1-B and -A, mouse HDAC1 and human HDAC1 and -4 enzymes. Effects on cell cycle, apoptosis, and differentiation of selected 2 and 3 derivatives in U937 cells at 24 and 48 h. This material is available free of charge via the Internet at <http://pubs.acs.org>.

■ AUTHOR INFORMATION

Corresponding Author

*Phone: +39 06 49913392. Fax: +39 06 49693268. E-mail: antonello.mai@uniroma1.it.

Notes

The authors declare no competing financial interest.

■ ACKNOWLEDGMENTS

This work was supported by FIRB RBFR10ZJQT, Italian Association for Cancer Research (MFAG no. 11502), Progetto Ateneo Sapienza 2013, Progetto IIT-Sapienza, RF-2010-2318330, and FP7 projects BLUEPRINT/282510 and A-ParaDDisE/602080.

■ ABBREVIATIONS USED

AML, acute myeloid leukemia; AR, androgen receptor; CD11c-PE, phycoerythrin-conjugated CD11c; CTCL, cutaneous T-cell lymphoma; ER α , estrogen receptor α ; FACS, fluorescence activated cell sorting; HAT, histone acetyltransferase; HDAC, histone deacetylase; HIF-1 α , hypoxia-inducible factor 1 alpha; HSP90, heat shock protein 90; NF- κ B, nuclear factor- κ B; PBS, phosphate buffered saline; PI, propidium iodide; SAHA, suberoylanilide hydroxamic acid; Smad7, mothers against decapentaplegic homologue 7; Stat3, signal transducer and activator of transcription 3

■ REFERENCES

- (1) Clayton, A. L.; Hazzalin, C. A.; Mahadevan, L. C. Enhanced histone acetylation and transcription: a dynamic perspective. *Mol. Cell* **2006**, *23*, 289–296.
- (2) Glozak, M. A.; Sengupta, N.; Zhang, X.; Seto, E. Acetylation and deacetylation of non-histone proteins. *Gene* **2005**, *363*, 15–23.
- (3) Mai, A. Small-molecule chromatin-modifying agents: therapeutic applications. *Epigenomics* **2010**, *2*, 307–324.
- (4) Benedetti, R.; Conte, M.; Altucci, L. Targeting HDACs in diseases: where are we? *Antioxid. Redox Signaling* **2014**, Mar 6, PMID 24382114, DOI 10.1089/ars.2013.5776.
- (5) Marks, P. A.; Breslow, R. Dimethyl sulfoxide to vorinostat: development of this histone deacetylase inhibitor as an anticancer drug. *Nature Biotechnol.* **2007**, *25*, 84–90.
- (6) Campas-Moya, C. Romidepsin for the treatment of cutaneous T-cell lymphoma. *Drugs Today* **2009**, *45*, 787–795.
- (7) Mai, A.; Massa, S.; Rotili, D.; Cerbara, L.; Valente, S.; Pezzi, R.; Simeoni, S.; Ragno, R. Histone deacetylation in epigenetics: an attractive target for anticancer therapy. *Med. Res. Rev.* **2005**, *25*, 261–309.
- (8) Li, J.; Li, G.; Xu, W. Histone deacetylase inhibitors: an attractive strategy for cancer therapy. *Curr. Med. Chem.* **2013**, *20*, 1858–1886.
- (9) Valente, S.; Conte, M.; Tardugno, M.; Massa, S.; Nebbioso, A.; Altucci, L.; Mai, A. Pyrrole-based hydroxamates and 2-aminoanilides: histone deacetylase inhibition and cellular activities. *ChemMedChem* **2009**, *4*, 1411–1415 and references cited therein..
- (10) Valente, S.; Tardugno, M.; Conte, M.; Cirilli, R.; Perrone, A.; Ragno, R.; Simeoni, S.; Tramontano, A.; Massa, S.; Nebbioso, A.; Miceli, M.; Franci, G.; Brosch, G.; Altucci, L.; Mai, A. Novel cinnamyl hydroxyamides and 2-aminoanilides as histone deacetylase inhibitors: apoptotic induction and cytodifferentiation activity. *ChemMedChem* **2011**, *6*, 698–712 and references cited therein..
- (11) Mai, A.; Perrone, A.; Nebbioso, A.; Rotili, D.; Valente, S.; Tardugno, M.; Massa, S.; De Bellis, F.; Altucci, L. Novel uracil-based 2-aminoanilide and 2-aminoanilide-like derivatives: histone deacetylase inhibition and in-cell activities. *Bioorg. Med. Chem. Lett.* **2008**, *18*, 2530–2535 and references cited therein..
- (12) Lahm, A.; Paolini, C.; Pallaoro, M.; Nardi, M. C.; Jones, P.; Neddermann, P.; Sambucini, S.; Bottomley, M. J.; Lo Surdo, P.; Carfi,

A.; Koch, U.; De Francesco, R.; Steinkühler, C.; Gallinari, P. Unraveling the hidden catalytic activity of vertebrate class IIa histone deacetylases. *Proc. Natl. Acad. Sci. U. S. A.* **2007**, *104*, 17335–17340.

(13) Trisciuglio, D.; Ragazzoni, Y.; Pelosi, A.; Desideri, M.; Carradori, S.; Gabellini, C.; Maresca, G.; Nescatelli, R.; Secci, D.; Bolasco, A.; Bizzarri, B.; Cavaliere, C.; D'Agnano, I.; Filetici, P.; Ricci-Vitiani, L.; Rizzo, M. G.; Del Bufalo, D. CPTH6, a thiazole derivative, induces histone hypoacetylation and apoptosis in human leukemia cells. *Clin. Cancer Res.* **2012**, *18*, 475–486.

(14) Nebbioso, A.; Manzo, F.; Miceli, M.; Conte, M.; Manente, L.; Baldi, A.; De Luca, A.; Rotili, D.; Valente, S.; Mai, A.; Usiello, A.; Gronemeyer, H.; Altucci, L. Selective class II HDAC inhibitors impair myogenesis by modulating the stability and activity of HDAC-MEF2 complexes. *EMBO Rep.* **2009**, *10*, 776–782.

(15) Nebbioso, A.; Clarke, N.; Voltz, E.; Germain, E.; Ambrosino, C.; Bontempo, P.; Alvarez, R.; Schiavone, E. M.; Ferrara, F.; Bresciani, F.; Weisz, A.; de Lera, A. R.; Gronemeyer, H.; Altucci, L. Tumor-selective action of HDAC inhibitors involves TRAIL induction in acute myeloid leukemia cells. *Nature Med.* **2005**, *11*, 77–84.

(16) Altucci, L.; Rossin, A.; Raffelsberger, W.; Reitmair, A.; Chomienne, C.; Gronemeyer, H. Retinoic acid-induced apoptosis in leukemia cells is mediated by paracrine action of tumor-selective death ligand TRAIL. *Nature Med.* **2001**, *7*, 680–686.

(17) Valente, S.; Trisciuglio, D.; Tardugno, M.; Benedetti, R.; Labella, D.; Secci, D.; Mercurio, C.; Boggio, R.; Tomassi, S.; Di Maro, S.; Novellino, E.; Altucci, L.; Del Bufalo, D.; Mai, A.; Cosconati, S. *tert*-Butylcarbamate-containing histone deacetylase inhibitors: apoptosis induction, cytodifferentiation, and antiproliferative activities in cancer cells. *ChemMedChem* **2013**, *8*, 800–811.